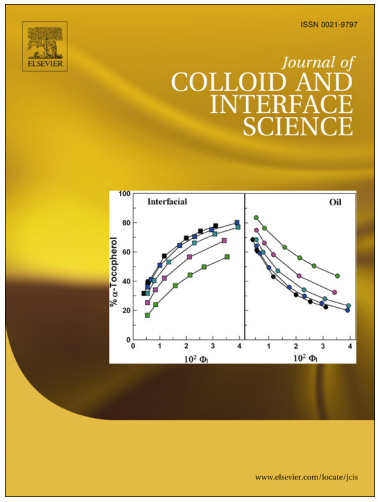

Conditioning materials with biomacromolecules: Composition of the adlayer and influence on cleanability

Yetioman Touré, Michel J. Genet, Christine C. Dupont-Gillain, Marianne Sindic, Paul G. Rouxhet

PII: S0021-9797(14)00380-4
DOI: http://dx.doi.org/10.1016/j.jcis.2014.06.002
Reference: YJCIS 19618

To appear in: *Journal of Colloid and Interface Science*

Received Date: 13 March 2014
Accepted Date: 3 June 2014

Please cite this article as: Y. Touré, M.J. Genet, C.C. Dupont-Gillain, M. Sindic, P.G. Rouxhet, Conditioning materials with biomacromolecules: Composition of the adlayer and influence on cleanability, *Journal of Colloid and Interface Science* (2014), doi: http://dx.doi.org/10.1016/j.jcis.2014.06.002

Conditioning materials with biomacromolecules: Composition of the adlayer and influence on cleanability

Yetioman Touré[a], Michel J. Genet[b], Christine C. Dupont-Gillain[b], Marianne Sindic[a], Paul G. Rouxhet[b]*

[a]Laboratory of Agro-food Quality and Safety, Analysis Quality and Risk Unit, University of Liège-Gembloux Agro-Bio Tech, Passage des Déportés 2, B-5030 Gembloux, Belgium. Email: yetiomantiti@yahoo.fr / yetioman.toure@doct.ulg.ac.be, marianne.sindic@ulg.ac.be

[b]Institute of Condensed Matter and Nanosciences - Bio & Soft Matter, Université catholique de Louvain, Croix du Sud 1/L7.04.01, B-1348 Louvain-la-Neuve, Belgium. Email: michel.genet@uclouvain.be, christine.dupont@uclouvain.be, paul.rouxhet@uclouvain.be

*_Coresponding author_: Paul G. Rouxhet; _Email_: Paul.rouxhet@uclouvain.be

Post address: Institute of Condensed Matter and Nanosciences - Bio & Soft Matter, Université catholique de Louvain, Croix du Sud 1/L7.04.01, B-1348 Louvain-la-Neuve, Belgium. _Telephone_: +32-10-47 35 87, 32-10-47 35 89, _Fax_: +32-10-47 20 05

Abbreviations

BSA: bovine serum albumin

RFC: radial flow cell

XPS: X-ray photoelectron spectroscopy

ABSTRACT

The influence of substrate hydrophobicity and biomacromolecules (dextran, bovine serum albumin - BSA) adsorption on the cleanability of surfaces soiled by spraying aqueous suspensions of quartz particles (10 to 30 µm size), then dried, was investigated using glass and polystyrene as substrates. The cleanability was evaluated using radial flow cell (RFC). The surface composition was determined by X-ray photoelectron spectroscopy (XPS). The interpretation of XPS data allowed the complexity due to the ubiquitous presence of organic contaminants to be coped with, and the surface composition to be expressed in terms of both the amount of adlayer and the mass concentration of adlayer constituents.

When soiled with a suspension of particles in water, glass was much less cleanable than polystyrene, which was attributed to its much lower water contact angle, in agreement with previous observations on starch soil. Dextran was easily desorbed and did not affect the cleanability. The presence of BSA at the interface strongly improved the cleanability of glass while the contact angle did not change appreciably. In contrast, soiling polystyrene with quartz particles suspended in a BSA solution instead of water did not change markedly the cleanability, while the contact angle was much lower and the aggregates of soiling particles were more flat. These observations are explained by the major role of capillary forces developed upon drying, which influence the closeness of the contact between the soiling particles and the substrate and, thereby, the adherence of particles. The capillary forces are proportional to the liquid surface tension and depend in a more complex way on contact angles of the particles and of the substrate. The dependence of cleanability on capillary forces, and in particular on the liquid surface tension, is predominant as compared with its dependence on the size and shape of the soiling aggregates, which influence the efficiency of shear forces exerted by the flowing water upon cleaning.

Keywords: Fouling; Cleaning; Particulate soiling; Protein adsorption; Polysaccharide adsorption; Radial-flow cell; XPS; Capillary forces

1. Introduction

Fouling is the accumulation of unwanted matter on surfaces of materials. The fouling matter may consist of living organisms (biofouling). Non-living fouling has been classified according to different criteria for understanding the formation of deposit and the principles of cleaning: chemical, particulate, crystallization, corrosion, organic, mineral, composite soils (Fryer and Asteriadou, 2009). Particulate fouling may occur when particles settle out onto the substrate by splashing of a suspension or by sedimentation, e.g. of particles (clays, oxides, protein aggregates, etc) suspended in aqueous media or dust from air. Cleaning is an important issue in food and pharmaceutical industries. Its efficiency influences the final quality of the products, and is crucial to insure the absence of cross-contaminations and batch integrity (Stephan et al., 2004). The presence of adhering particles and microorganisms is also undesirable after cleaning and disinfection of open surfaces in applications where hygiene is critical.

Hydrodynamic effects are crucial for the cleaning efficiency, through the shear stress forces acting at the equipment walls (Lelièvre et al., 2002; Jensen et al., 2005; Blel et al., 2007). However, the wall shear stress, mainly governed by the flow rate and the equipment design, is not the only factor explaining cleaning performance. Physico-chemical processes at interfaces created at different stages of fouling and cleaning may be important (Jensen et al., 2007 ; Detry et al., 2009a; Blel et al., 2010). Under this respect, typical examples are fouling with particles (Määttä et al., 2011; 2007; Detry et al., 2011; Pesonen-Leinonen et al., 2006a; 2006b; Kuisma et al., 2007) and with a continuous layer of more or less complex composition (Mauermann et al., 2009; 2011; Piispanen et al., 2011), but these two situations differ according to the influence of the substrate surface properties on drying and cleaning. The interactions between the substrate and particulate contaminants need to be better understood in order to reduce equipment fouling, to improve the efficiency of cleaning and disinfection, or to develop easy-to-clean surfaces (Podczeck, 1999). Chemical compounds present in food and pharmaceutical mixtures may influence interactions with surfaces and adhesion processes (Speranza et al., 2004). Proteins at the outer surface of bacteria are known to play an important role in the initial attachment to solid surfaces in water (Dufrêne et al., 1996; Flint et al., 1997; Caccavo, 1999; Boonaert and Rouxhet, 2000; Lower et al., 2005; Mercier-Bonin et al., 2009). In a work devoted to soiling by starch suspension, it was reported (Detry et al., 2011) that the presence of macromolecules, mainly polysaccharides, which were adsorbed

from the liquid phase or carried by the retracting water film and deposited at the granule-substrate interface, acted as an adhesive joint, the properties of which seemed to be influenced by the detailed history of drying and subsequent exposure to humidity. Macromolecules dissolved in the starch suspension may act in various ways: (i) modification of liquid surface tension and drop spreading upon soiling, (ii) adsorption at the solid-liquid interface, (iii) accumulation at substrate-particulate interface upon drying. In a previous study, (Touré et al., 2011), we showed that conditioning polystyrene substrate with dextran (80 mg/L) slightly increased the adherence of quartz particles and that the opposite occurred when conditioning glass substrate with dextran, whether quartz particles were or not conditioned with dextran themselves. However the presence of dextran preserved the large difference between polystyrene and glass regarding droplet spreading, aggregation of soiling particles and cleanability.

The aim of the present study is to improve the understanding of mechanisms affecting soiling and cleanability by comparing the influence of polysaccharides and proteins on hydrophilic and hydrophobic substrates. Therefore, a particular effort was made to analyze the surfaces by X-ray photoelectron spectroscopy (XPS), coping with the complexity due the ubiquitous presence of organic contaminants at the surface of high energy solids. Quartz particles were kept as a simplified particulate soil model. Glass and polystyrene were chosen as model substrates to examine the influence of substrate hydrophobicity. Dextran is a model of soluble polysaccharide available with a defined molecular size. Bovine serum albumin (BSA) was chosen because it is the common soluble protein used for laboratory studies, and has surfactant properties. It is a globular and structurally labile (soft) protein, which may change its conformation upon adsorption (Norde and Giacomelli 2000; Kopac et al., 2008). The influence of macromolecules was examined by involving them in two ways, introducing them into the quartz suspension used for soiling or conditioning the substrates with them prior to soiling.

2. Experimental

2.1. Substrates and chemicals

Glass slides were purchased from Menzel-Gläser (Germany); the bulk composition was 72.2% SiO_2, 14.3% Na_2O, 1.2% K_2O, 6.4% CaO, 4.3% MgO, and 1.2% Al_2O_3. Slides of 50 mm × 50 mm × 1 mm size were used for soiling and cleaning experiments; slides of 37 mm × 16 mm × 1 mm size were used for surface characterization, either as such for contact angle measurement or after being cut to 16 mm × 10 mm for XPS analysis. Polystyrene sheets (300

mm × 300 mm × 0.25 mm) were purchased from Goodfellow (United Kingdom) and cut to the desired dimensions (50 mm × 50 mm, 37 mm × 16 mm or 16 mm × 10 mm) according to the need.

MilliQ water was produced by a MilliQ-50 system from Millipore (France). The chemical products used were ethanol 96%, sulfuric acid (98%), hydrogen peroxide solution (30%) purchased from Sigma-Aldrich (Wisconsin, USA) and RBS 50 cleaning agent (Chemical Products R. Borghgraef, Belgium). Dextran from *Leuconostoc mesenteroides,* (20% w/w solution, molar mass 500000 g/mol) and albumin from bovine serum (BSA) (lyophilized powder, ≥ 98%, essentially fatty acid free, essentially globulin free, molar mass 66000 g/mol) were purchased from Sigma-Aldrich (Wisconsin, USA).

2.2. Substrate conditioning

Before use, the glass substrates were cleaned by immersion for 10 min at 50°C in an alkaline detergent solution (RBS 50 diluted 50 times; pH 11.9) and sonicated for 10 min in ultrasonic cleaner (Branson 3200, USA) to remove dust particles. The samples were then rinsed with MilliQ water and cleaned by immersion in a "piranha mixture" (sulfuric acid / hydrogen peroxide 2/1 v/v) at room temperature for 10 min and rinsed thoroughly with MilliQ water.

Polystyrene substrates were first cleaned with ethanol, dried with Kimtech Science paper (Kimberly–Clark, United Kingdom) and immersed for 30 min in ethanol. They were then rinsed thoroughly with MilliQ water.

Both glass and polystyrene substrates were dried with a gentle flow of nitrogen and wrapped in an aluminum foil. The substrates were used as such or conditioned by immersion for 1 h in a 8 g/L dextran or BSA solution at room temperature (volume of 150 mL for the 50 x 50 mm slides, 10 mL for smaller slides). The conditioned slides intended for XPS analysis were rinsed using a procedure which avoided repeated formation of water-air meniscus in contact with the adsorbed phase. Therefore the slide was not repeatedly taken out of the liquid but the solution was diluted, removing of 8 ml from the 10 ml of the solution and adding 8 ml of MilliQ water, with time intervals of 5 min between rinsing steps. When finally taken out of the liquid, the substrates were flushed with nitrogen for removing the liquid film and wrapped in aluminum foil until use for soiling or placed in a Petri dish for XPS analysis. In the latter case, the conditioned substrates were examined as such, or rinsed once or three times before drying as described in section 2.6.4. The concentration of 8 g/L chosen for BSA is lower than the protein concentration in egg white and blood plasma (about 100 g/L from which about 50% albumin, http://en.wikepedia.org); it is slightly higher compared to the whey protein concentration in cow milk (6 g/L, Walstra and Jenness, 1984) and to the BSA concentration at

which adsorption by silica and polystyrene latex reaches a plateau (Norde and Giacomelli, 2000). The dextran concentration was chosen to be the same as that of BSA; this might possibly enhance adsorption with respect to the much lower concentration used previously (Touré et al., 2011), which affected only slightly cleanability.

2.3. Soil preparation

Ground quartz was provided by Sibelco Benelux (Belgium). The material was M400, characterized by a particle size distribution of 1.1 to 60.3 µm. A narrower size distribution (target 10 to 30 µm) was isolated from the initial batch by repeated sedimentation. The particle size distribution (Mastersizer 2000, Malvern Instruments, United Kingdom) of the isolated fraction was unimodal, ranging from 7.6 to 32.7 µm diameter (D10%=10.6 µm; D50%=17.1 µm; D90%=27.1 µm).

Three kinds of quartz suspensions were prepared at a concentration of 150 g/L: (i) in MilliQ water, (ii) in a dextran solution (8 g/L), (iii) in a BSA solution (8 g/L). For preparing the suspensions in dextran and BSA solutions, 7.5 g of quartz were first mixed with 25 ml of MilliQ water and stirred for 30 min at room temperature. Then, 25 ml of a dextran or BSA solution in MilliQ water (16 g/L) were added and the entire mixture was stirred for 1h. The suspensions were kept at 4°C, which was the temperature of dextran and BSA storage, for 72h.

2.4. Soiling procedure

The glass and polystyrene substrates (size 50 mm x 50 mm) were soiled with the quartz suspensions brought at room temperature, by manual aspersion using a thin layer chromatography (TLC) sprayer located 40 cm from the substrate (Detry et al.; 2007; 2011). This did not lead to formation of a continuous liquid film and no drainage occurred. The substrates were dried for 30 min in a dark cupboard at 20.6±1.9°C, with a relative humidity 39±3%. The specifications of these conditions were determined with a Testo 175-H2 logger (Testo, Germany) during three weeks and were in agreement with previous records (Detry et al. 2007; 2011).

2.5. Cleaning experiments

Cleaning experiments were performed in a radial flow cell (RFC). This consisted of an upper disk with a 2 mm diameter central inlet and a lower disk in which the soiled square sample was fitted to be cleaned. The distance between the upper disk and both the sample and the lower disk was set by three adjustable micrometric screws and controlled to be 1.00±0.02 mm with calibrated steel spacers. A complete description of the device and of its hydrodynamics can be found elsewhere (Detry et al., 2009b). The cleaning fluid used was distilled water and

cleaning was performed at 20°C at controlled flow rates (40 or 390 ml/min) for 5 min. The flow rate was selected with the aim of comparing samples, according to previous studies (Detry et al. 2007; 2011). The sample was then removed and dried at room temperature. Pictures of the substrate were taken before and after cleaning, using an epifluorescence stereomicroscope (ZX9 Olympus, Belgium) equipped with a CCD camera, a mercury vapour UV lamp (100W, emission range 100-800 nm) and UV filters (passing bands: excitation 460-490 nm, emission > 520 nm). After cleaning, a circular zone with a lower density of aggregates was observed at the center of the sample. The pictures of the sample before and after cleaning were processed with a specific application of the Matlab software (The Mathworks Inc.), which gave the ratio of the number of aggregates initially present on the surface to the number of aggregates remaining after cleaning, as a function of the radial position. The radial position at which the residual density of aggregates was half the initial density was considered as the critical detachment radius (Goldstein and Dimilla 1997; 1998). The value of the critical radius was checked for consistency in the LUCIA G image analysis software (LIM, Prague, Czech Republic) to insure the absence of artifacts such as the nucleation of air bubbles on the surface. At least 10 repetitions of each experiment (soiling-cleaning) were made, being distributed in at least three independent series. Experiments at different flow rates were performed on different soiled samples. The error bars show the standard deviations.

2.6. Methods of characterization

2.6.1. Scanning electron microscopy (SEM)

The surface of soiled samples was examined by scanning electron microscopy (DSM 982 Gemini from Leo, field-effect gun) in secondary electrons mode (external detector) and backscattered electrons mode (in-lens detector). The images presented here were obtained using an accelerating voltage of 1 kV. Samples were examined after deposition of a 10 nm-thickness chromium coating.

2.6.2. Optical microscopy

Optical micrographs (20X objective) of soiled polystyrene were submitted to image analysis using LUCIA G image analysis software (LIM, Prague, Czech Republic). For each type of sample, two slides (50 x 50 mm^2) were examined. For each slide, five fields (1 field = 0.25 cm^2) were chosen randomly and a picture was taken at a random place in each field (one picture corresponding to 0.52 mm^2). The equivalent diameter of entity contours was determined based on their measured area and using and Eq. (1):

$$\text{diameter} = 2(\text{area} / \pi)^{1/2} \qquad (1)$$

The entity contours were defined using three different threshold gray levels: 40, 90 and 180. For each threshold, data were exported into a txt-file and processed using an Excel tool, providing the size distribution, i.e. the number of objects per class size defined as ≤ 30 µm, 30 to 90 µm and > 90 µm.

2.6.3. Contact angle and liquid surface tension

Static contact angles of water, dextran solution, BSA solution, and supernatants of quartz particles on the substrates were measured using the sessile drop method with a goniometer (Krüss, Germany). Advancing and receding contact angles of water were determined by recording wetting curves (cycles of immersion and emersion) using the Wilhelmy plate method (Tensiometer K100, Krüss, Germany); therefore the effect of buoyancy was corrected and the records were made as a function of the position of the three-phase contact line on the sample slide (Tomasetti et al., 2013). The surface tension of the liquids was measured with a Prolabo Tensiometer (Tensimat n°3) using the Wilhelmy plate method. All these measurements were performed at room temperature.

2.6.4. X-ray photoelectron spectroscopy

Slides of about 16 mm × 10 mm were used for surface analysis by X-ray photoelectron spectroscopy (XPS). The substrates were analyzed either (i) just cleaned; (ii) conditioned by immersion for 1 h in a 8 g/L dextran or BSA solution at room temperature; (iii) same as (ii) and then rinsed once or three times. The analysis was also performed on quartz samples obtained by freeze drying (i) the sediment collected from a suspension (150 g/L) in MilliQ water; (ii) the sediment from suspension (150 g/L) in dextran or BSA solution (8 g/L); (iii) the sediment as (ii), rinsed twice, three times or four times by sedimentation and replacement of the supernatant by water. The final sediments were stored at 4°C for 72 h before being frozen. Finally, dextran and BSA thick layers were also analyzed. These were prepared by successively drying 5 drops of a solution in water deposited on polystyrene.

Both glass and polystyrene samples were fixed on a standard stainless steel holder by using a piece of double-sided insulating tape. Quartz powders (from freeze-dried sediments) were placed in a stainless steel trough with an inner diameter of 4 mm and mildly pressed with a polyacetal surface cleaned with isopropanol, to obtain a smooth surface.

The XPS analyses were performed with a SSX 100/206 X-ray photoelectron spectrometer from Surface Science Instruments (USA) equipped with a monochromatized micro-focused Al X-ray source (powered at 20 mA and 10 kV). A flood gun set at 6 eV and a Ni grid placed 3 mm above the sample surface were used for charge stabilization. The pressure in the analysis chamber was about 10^{-6} Pa. The angle between the normal to the surface and the axis

of the analyzer lens was 55°. The analyzed area was approximately 1.4 mm^2 and the pass energy was set at 150 eV for the survey spectrum and 50 eV for high energy resolution spectra. In the latter conditions, the full width at half maximum (FWHM) of the Au $4f_{7/2}$ peak of a clean gold standard sample was about 1.1 eV. The following sequence of spectra was recorded: survey spectrum, C 1s and K 2p (glass samples only), O 1s, N 1s, Si 2p, S 2p (on some samples treated with BSA) and C 1s again to check for sample charging stability and absence of sample degradation.

The binding energy scale was set by fixing the C 1s component due to carbon bound only to carbon and hydrogen at 284.8 eV. The data analysis was performed with the CasaXPS program (Casa Software, Teignmouth, UK). Molar concentration ratios were calculated from peak areas (linear background subtraction) normalized on the basis of the acquisition parameters and of sensitivity factors and transmission function provided by the manufacturer. The C 1s peak was decomposed by using a least square fitting procedure with a 85:15 Gaussian-Lorentzian product function. The linear regression equations between spectral data were computed using Excel software.

3. Results

3.1. Surface cleanability

The critical radius of detachment, which was the output of the cleaning experiments, is related to a critical wall shear stress and the minimal hydrodynamic drag force required to detach particles in the given experimental conditions (Jensen and Friis, 2004). However, recent studies showed that the conversion of critical radius into critical wall shear stress may be biased when the adhering aggregate height is not negligible with respect to the channel height and when the adherence is such that flow rates above 20 ml/min are required (Detry et al. 2007; 2009a). Owing to these limitations, this conversion was not made here, but it may be kept in mind that a higher adherence was revealed by a lower critical radius at a given flow rate, and by a larger flow rate for a given critical radius.

Figure 1A presents the critical detachment radii measured for the substrates, conditioned or not with dextran, soiled with a quartz suspension in water or in a dextran solution. For glass, no detachment radius could be measured after cleaning at a flow rate of 40 ml/min, indicating that the shear stress generated at this flow rate was not high enough to provoke particle detachment. Therefore a flow rate of 390 ml/min was used; this shows that the presence of dextran decreased slightly the adherence. For polystyrene, the detachment radius was larger than the microscope view field when the flow rate was 390 ml/min, indicating a much higher

cleanability compared to glass. In order to examine the influence of conditioning, the detachment radii were measured by setting the flow rate at 40 ml/min. The presence of dextran in the quartz suspension did not influence the adherence, but conditioning the substrate with dextran led to a slight increase of the adherence.

Figure 1B presents the critical detachment radii measured for the substrates, conditioned or not with BSA, soiled with a quartz suspension in water or in a BSA solution. For both substrates, the detachment radii could be compared after cleaning at flow rates of 40 ml/min. For polystyrene substrate, the detachment radius was not significantly influenced by the presence of BSA, whether due to substrate conditioning or to the quartz suspension medium. In contrast, the presence of BSA increased dramatically the critical detachment radius for the glass substrate, and thus decreased the adherence, leading to values beyond those observed for polystyrene.

3.2. Soil morphology

Representative optical and SEM micrographs of the soiled substrates before cleaning are presented in Figure 2 for the different systems investigated. When polystyrene was not conditioned with BSA, the SEM images showed that many quartz particles formed dense rounded aggregates. For glass and BSA-conditioned polystyrene, particles were more dispersed or formed elongated motifs. The presence of more numerous coarse aggregates on bare or dextran-conditioned polystyrene was also revealed by optical micrographs.

The micrographs of Figure 2 are representative of observations made. In order to test the significance of differences between samples, the optical micrographs obtained on polystyrene were studied in more detail by image analysis. The detailed results are shown in Supporting Material (Table S1) in the form of the density of objects and their distribution in 3 size fractions: ≤ 30 µm, 30 to 90 µm, > 90 µm. Increasing the threshold led to an increase of the small size fraction and a decrease of the large size fraction. Using a threshold of 180 decreased the number of counted objects and the decrease was much stronger for the two systems involving BSA. In Figure 2B, the images obtained with a threshold of 180 can be compared with the direct micrographs and provide a clear evidence of lower aggregation of particles on polystyrene soiled in the presence of BSA.

Combination of SEM and optical microscopy thus showed that particles were more aggregated on bare and dextran-conditioned polystyrene compared to glass samples and to BSA-conditioned polystyrene. The situation was less clear and possibly intermediate in the case of bare polystyrene soiled with a suspension of quartz in a BSA solution.

3.3. Contact angle

Figure 3A presents the contact angles measured on the substrates, conditioned or not with dextran, using the supernatant of a quartz suspension in water or in a dextran solution, or using a dextran solution. The results show that the great difference between glass and polystyrene was maintained in all conditions (substrate conditioned or not, presence of dextran or not in the solution, supernatant or pure solution). They also show that conditioning the substrates with dextran (b, d and f compared to a, c and e) led to a slight increase of the contact angle, irrespective of the liquid used.

Figure 3B show analogous results obtained with BSA instead of dextran. Conditioning glass with BSA (b, d, f) led to a very slight increase of the contact angle, which remained however in the range of 10 to 20°. On the other hand, conditioning polystyrene with BSA provoked a strong decrease of the contact angle, from the range of 80 to 85° to the range of 25 to 30°. The contact angle measured with a solution containing BSA (pure solution or supernatant) was not markedly different from that measured with pure water.

3.4. Liquid surface tension

Table 1 presents the surface tensions of water, of dextran and BSA solutions and of supernatants of quartz particles suspensions in water and in dextran and BSA solutions. There was no significant difference between the surface tension of water, dextran solution and supernatant of quartz suspension in water. The surface tension of the supernatant of the quartz suspension in dextran solution was slightly lower. The presence of BSA in the liquid phase markedly decreased the surface tension, giving 30 and 49 mN/m for the BSA solution and for the supernatant of the quartz suspension in BSA solution, respectively.

3.5. Surface composition

Table 2 gives the surface elemental composition determined by XPS on the residue obtained after evaporation of drops of dextran and BSA solution, on bare substrates, on conditioned substrates, rinsed or not, on quartz powder collected from a suspension in water, and on quartz powder conditioned by suspension in a dextran or BSA solution, and rinsed or not. The presence of oxygen, oxidized carbon and silicon at the surface of non-conditioned polystyrene may explain that the water contact angle (Figure 3) was lower than expected (Dupont-Gillain et al., 2000). Figure 4 presents representative O 1s, N 1s and C 1s peaks recorded with the siliceous solids. Non-conditioned glass and quartz showed the presence of carbon. This was attributed to organic contaminants which were not removed by the cleaning procedure or were adsorbed from the surrounding, either the ambient atmosphere or the spectrometer vacuum chambers (Rouxhet, 2013).

The C 1s peak was decomposed (Rouxhet et al., 2008; Rouxhet and Genet, 2011), allowing the possibility of 4 components, in addition to the shake up contribution at 291.4 eV (C_{sh}) observed in the case of samples with polystyrene substrate. The full width at half maximum was imposed to be the same for the 4 components. No constraint was imposed on the binding energy of the components except when their intensity was very weak, in which case the binding energy was constrained to be in range observed otherwise. The component attributed to carbon only bound to carbon and hydrogen [**C**-(C,H)] was set at 284.8 eV. Other components were found at 286.3 ± 0.2 eV, assigned to carbon making a single bond with oxygen or nitrogen [**C**-(O,N)], and 288.0 ± 0.2 eV, assigned to carbon making one double or two single bonds with oxygen, typical of amide function in proteins [N-**C**=O] and of acetal link in polysaccharides [O-**C**-O], respectively. For certain samples, a very weak component was found near 289.3 eV, which may be due to ester or carboxyl. The results of the C 1s peak decomposition are presented in Table 2.

The O 1s peak was found at 532.6 eV for dextran [C-**O**H, C-**O-**C], and had a maximum near 531.4 eV for BSA [N-C=**O**]. Glass and quartz powder showed an O 1s peak at 532.7 eV and 532.3 eV, respectively. The position and shape of the O1s peak of conditioned samples varied according to the respective contributions. Its decomposition was not performed, owing to the overlap of the contribution of siliceous solids with that of the organic adlayer, particularly dextran.

The main N 1s peak at 399.0 - 400.0 eV and a minor component, typically 20 times less intense, near 402 eV were attributed to amide or non-protonated amine and to protonated amine, respectively. For samples showing a high N concentration, a S 2p doublet was found with the S $2p_{3/2}$ component near 163.7 eV, which was attributed to sulfur-containing residues of BSA (Caillou et al., 2007).

The Si 2p peak of glass and quartz samples was found near 103.0 eV. Silicon was detected in low concentration on polystyrene samples and attributed to surface contamination. Glass samples showed a Na 1s peak near 1071.5 - 1072.0 eV. Non-conditioned glass also showed low concentrations of calcium (about 1%), potassium (about 0.25%) and chloride (about 0.25%) but these peaks were not recorded after conditioning.

Extraction of meaningful information from XPS spectra is complicated by several features: presence of organic contaminants in addition to expected adsorbate, overlap of solid and adsorbate contributions in the C1s peak of polystyrene samples and in the O 1s peak of siliceous samples. On the other hand, peak decomposition is an interpreting approach which involves a trade-off between imposing constraints and generating information (Rouxhet and

Genet, 2011). Correlations between independent spectral data (elements, C 1s peak components) were used to validate peak decomposition and component assignment, and to identify useful markers for the determination of surface molecular composition. Therefore reference data were deduced from the amino acid sequence of BSA (Hirayama et al., 1990) and are presented in Supporting Material. They concern the elemental composition as well as the chemical functions associated with the components of the C 1s and O 1s peaks and their concentrations.

Figure 5a presents the correlation between the concentration of carbon in an oxidized form

$$C_{ox} = C_{tot} - C_{284.8} - C_{sh} \quad (2)$$

and the concentration of nitrogen, N, for all samples except those involving dextran: non-conditioned solids, BSA and solids conditioned with BSA. The regression line was computed without considering the non-conditioned solids and provided a slope of 1.99, close to the value of 2.01 expected for BSA (details in Supporting Material). The intercept was small, in agreement with data obtained for non-conditioned solids, and attributed to organic contaminants present on glass and quartz powder and to a slight oxidation of polystyrene surface. Correlations between the concentration of C_{288} (attributed to N-**C**=O) and $C_{286.3}$ (attributed to **C**-N) and the N concentration are shown in Supporting Material. A comparison with data expected for BSA indicates that the separation between these two components is less reliable than the separation between the contributions of C_{ox} and $C_{284.8.}$

Dextran and dextran-conditioned solids showed a small concentration of nitrogen, which was not observed for non-conditioned solids (Table 2). This was attributed to contamination of the glass vessels by proteins, presumably BSA. The contribution of BSA to the concentrations should be $C_{ox\text{-}BSA}$ = 2.01*N and O_{BSA} = 1.15*N (details in Supporting Material). The concentration ratio (C_{ox} -2.01*N)/(O- 1.15*N) = 1.24 (from Table 2) measured for dextran sample is in excellent agreement with the expected value of 1.20. The non-BSA contributions for conditioned samples may be due to dextran, for which the contributions should be O_{dextr} = $C_{ox\text{-}dextr}$/1.2, or to organic contaminants, for which the contributions should be O_{cont} = $C_{ox\text{-}cont}$ if oxidized carbon is present in the form of alcohol, aldehyde, ketone or ester functions. The concentration of organic oxygen can then be deduced as follows:

$$O_{org} = N*1.15 + (C_{ox} - 2.01*N)/1.2 = 0.83*C_{ox} - 0.52*N \quad (3)$$

if the non-protein adsorbate is pure dextran, or

$$O_{org} = N*1.15 + (C_{ox} - 2.01*N) = C_{ox} - 0.86*N \quad (4)$$

if the non-protein adsorbate is only contaminants.

The concentration of oxygen due to siliceous solids may then be evaluated as $O_{inorg} = O_{tot} - O_{org}$ and should be related to the concentration of the inorganic elements according to the formulas SiO_2 and Na_2O. The plot of O_{inorg}, evaluated by equation (4), vs. (2*Si + 0.5*Na) is presented in Figure 6 (regression equation y = 1.18 x - 3.7) and is close to the expected 1:1 relationship. It is not significantly different if O_{inorg} is evaluated using equation (3), which gives the regression equation y = 1.13 x - 0.07. The regression equations thus do not permit to decide whether organic oxygen other than that of protein is due to dextran or to contaminants.

The correlations presented in Figures 5 a and 6, concerning all solids, bare or conditioned with BSA, and siliceous solids, bare or conditioned with dextran, demonstrate that the C1s peak decomposition and components assignment are reliable. According to the amino acid composition of BSA (Supporting Material), its contribution to carbon concentration is expected to be $C_{ox\ BSA} = 2.01*N$, in agreement with Figure 5a, $C_{284.8\text{-}BSA} = 1.75*N$ and $C_{tot\text{-}BSA} = 3.76*N$. Plots based on these considerations provide a direct visualization of the chemical nature of compounds other than BSA present at the surfaces, more specifically their relative content in oxidized carbon [C_{ox}] and carbon in the form of hydrocarbon moieties [**C**-(C,H)]. Polystyrene substrate must be excluded from these plots owing to the contribution of the substrate to the carbon peak.

Figure 5b presents the plot of ($C_{284.8} - 1.75*N$) vs ($C_{tot} - 3.76*N$) for BSA, and for glass and quartz powder, bare and conditioned with BSA. It shows that carbon which is not due to BSA is of hydrocarbon nature in a defined proportion of about 75%, in agreement with values reported for adventitious contamination (Gerin et al.., 1995). In the case of the BSA sample, the additional carbon may also be due to compounds which are present as traces in the BSA solution and accumulate at the liquid-air interface upon evaporation of the solution drop during sample preparation. It is indeed well known that the surface of solid food products is strongly enriched in lipids compared to proteins (Rouxhet and Genet, 2011). It may be noted in Figure 5b that the amount of carbon not due to BSA is much higher for bare siliceous solids than for BSA-conditioned siliceous solids. This suggests that BSA adsorption displaces organic contaminants present before conditioning or prevents contamination from the gas phase during sample handling in air and XPS analysis.

Figure 5c presents the plot of ($C_{ox} - 2.01*N$) vs ($C_{tot} - 3.76*N$) for dextran and for glass and quartz powder conditioned with dextran. It shows that carbon which was not due to BSA was mainly in oxidized form for non-rinsed dextran-conditioned samples. Most of dextran was

removed by rinsing, leaving an organic adlayer which contained a high proportion of hydrocarbon typical of contaminants, as revealed by Figure 5b.

It appears thus that N may be taken as a marker for BSA, ($C_{284.8}$ −1.75*N) may be taken as a marker for hydrocarbon moieties due to contaminants and, or to polystyrene, and (C_{ox} − 2.01*N) may be taken as a marker for dextran or oxidized carbon of contaminants.

4. Discussion

4.1. Surface composition

Ideally the surface composition should provide the adsorbed amount of each kind of adsorbate. The adsorbed amount should be expressed in mass per unit area or thickness of the adsorbed layer. This would require simulations based on models of the adsorbed layer involving hypothetical degrees of coverage and layer thicknesses, and would have a weak reliability owing to the complexity of the adsorbed layer and the lack of XPS measurements at different take-off angles. However comparisons of adsorbed amounts can be made between samples of the same solid, based on the sum of concentrations of elements due to the adsorbed layer, Σads, and due to the solid (glass or polystyrene substrate, or quartz powder), Σsol, which may be evaluated as follows, neglecting hydrogen. For siliceous samples,

$$\Sigma ads = C_{284.8} + 2*C_{ox} \quad (5)$$

where the second term provides an approximation for oxidized carbon, oxygen and nitrogen;

$$\Sigma sol = 3* Si + 1.5*Na \quad (6)$$

which accounts for inorganic elements and oxygen bound to them.

For polystyrene samples,

$$\Sigma ads = 5.91*N + 2*(C_{ox} - 2*N) \quad (7)$$

where the first term accounts for carbon, oxygen and nitrogen of BSA, while the second term provides an approximation for carbon and oxygen which are not due to BSA;

$$\Sigma sol = C_{284.8} + C_{sh} - 1.75*N \quad (8)$$

where the third term accounts for the part of $C_{284.8}$ due to BSA.

Table 3 (left part) gives the values of Σads and Σsol computed for the different samples. Conditioning the solids with BSA increased appreciably the importance of the organic adlayer, which was slightly decreased by subsequent rinsing. After conditioning with dextran, rinsing provoked a strong reduction of the contribution of the amount of adlayer.

In order to express the relative concentration of organic compounds at the surface (adlayer on siliceous solids, adlayer and substrate for polystyrene samples), the mass concentration of

molecular compounds is much more explicit than the molar concentration of elements. The relative mass concentration of organic compounds in the adsorbed layer may be computed from the mole fraction of markers and the related molar mass as recalled in Supporting Material (Table S5 and related text). In order to evaluate the mass % of non-BSA compounds, two models were considered, which differed according to hypotheses made regarding the relationship between oxygen and oxidized carbon. In model A, the compounds other than BSA were considered globally with the marker (C – 3.76*N), which accounts for carbon and hydrogen (in the form of CH_2 or H-C-OH), and (Cox – 2.01*N), which accounts for oxygen. In model B, the presence of dextran and hydrocarbon was considered, being accounted for by (Cox – 2.01*N) and ($C_{284.8}$ – 1.75*N), respectively. Application of model A to BSA-conditioned siliceous solids showed that BSA was the dominating constituent (about 90 mass % or above) in the adlayer and was not markedly removed by rinsing. In case of polystyrene samples, the same conclusion appeared based on the values of Σ_{ads}. For dextran-conditioned substrates, the two models A and B provided consistent results. Consideration of both Σ_{ads} and organic composition indicated that an appreciable amount of dextran was present at the surface of siliceous solids after conditioning but most of this was released upon rinsing. The amount of dextran present on dextran-conditioned polystyrene, even not rinsed, was not higher than the amount of protein.

4.2. Distribution of soiling particles and wetting properties

Conditioning glass with BSA slightly increased the contact angle, while conditioning polystyrene with BSA markedly decreased the contact angle (Figure 3B). It is noteworthy that the contact angle measured on bare polystyrene was not markedly affected by the presence of BSA in the liquid phase (compare a, c and e in Figure 3B). This is in relation with the measurement of the contact angle in advancing conditions, and the fact that BSA was not present on the surface to be wetted. The influence of protein adsorption and subsequent drying on the water contact angle was reported for several systems: non-annealed and annealed films of cellulose derivatives conditioned with BSA (Kosaka et al., 2005); silicon wafer, silanized silicon wafer and polystyrene conditioned with enolase (Almeida et al., 2002); set of materials with water contact angle ranging from 11 to 100° fouled with β-lactoglobulin and rinsed (Yang et al., 1991). In these works, protein conditioning of hydrophilic substrates led to an increase of the water contact angle while conditioning of hydrophobic substrates led to a decrease of the contact angle. The contact angle measured on most of these substrates after conditioning was in the range of 50 to 70°. The same trend was observed here. The water

contact angle measured after protein adsorption was however not higher than 20° for glass and 25 to 30° for polystyrene. The prefered orientation of certain amino acid residues at the surface of protein-conditioned substrates was demonstrated by Time-of-Flight Secondary Ion Mass Spectroscopy (Dupont-Gillain et al., 2010). In the case of hydrophobic substrates, protein adsorption may be driven by hydrophobic bonding, so that hydrophilic amino acids tend to be oriented toward water and remain so upon drying. In the case of hydrophilic substrates, the hydrophilic moieties should tend to get buried during drying in order to decrease surface energy. The fact that conditioned substrates fall in the same range of contact angles may be the consequence of the two mechanisms; however clarifying the relative importance of these mechanisms would require a comparison with the contact angle of thick protein layers. Under that respect, it may be noted that the results of Yang et al. (1991) covered a range of adsorbed amounts of 0.2 to 4 $\mu g/cm^2$, corresponding to a thickness about 1.4 to 28 nm, depending on the substrate. Accordingly they included adsorbed amounts which were much higher than one monolayer.

Conditioning glass with dextran slightly increased the contact angle (Figure 1B). This may be due to contamination with BSA as revealed by XPS, and is thus not significant. The influence of conditioning polystyrene with dextran was not significant.

On hydrophobic materials (polystyrene and dextran conditioned-polystyrene), particles were assembled in dense rounded aggregates (Figure 2). This was due to a lack of suspension droplet spreading: as water evaporated, particles were brought together and finally got compacted by capillary forces (Kralchevsky and Denkov, 2001; Kralchevsky and Nagayama K., 2001; 1994). On glass substrates and BSA conditioned-polystyrene, quartz particles were better dispersed, owing to spreading and coalescence of suspension droplets. As dewetting occurred, meniscuses were formed, and particles moved under the influence of lateral capillary forces, which led to the formation of aggregates in the form of elongated motifs (Thill and Spalla, 2003).

4.3. Cleanability

The lower cleanability of glass compared to polystyrene, when non-conditioned, (Figure 1a) is a robust observation, as it reproduces two previous independent observations (Touré et al., 2011; 2013). It may be explained by the lower contact angle (Figure 3a), in agreement with a study (Detry et al., 2011) of the adherence of starch granules on different substrates, including glass and polystyrene, using the same experimental approach as here (soiling with droplets of a starch suspension and drying, cleaning with the radial flow cell used in this work). A higher substrate wettability increases droplet spreading which leads to thinner aggregates and

decreases the efficiency of shear forces exerted by the flowing water. Moreover it enhances capillary forces at the interface between the particles and the substrate and insures a closer contact between their surfaces. As a result, the adherence of soiling particles is increased.

Literature data show that the wettability is important upon cleaning in air with a wet cloth, and may be related to the competition between substrate wetting and the capture of soiling particles by the liquid-air interface. The surface cleanability of materials soiled in air (rotating drum in a dry atmosphere in air) with a mix of inorganic particles (mainly quartz) presumably coated with paraffin oil was evaluated by the cleaning index (essentially ratio of soil removed by cleaning to initial soil), measured after cleaning with a microfiber cloth moistened with water, a solution of surfactant or a weakly alkaline model detergent (Pesonen-Leinonen et al., 2006a). The cleaning index decreased as the water contact angle of the substrate increased. Surface cleanability was also investigated (Määttä et al., 2007; 2011) using a soil model made of a suspension of chromium oxide or chromium acetyl acetonate particles in 1-propanol containing triolein, and cleaning with a microfiber cloth moistened with a detergent solution. For all substrates, the removal of chromium oxide was more efficient compared to the organic salt. A more detailed influence of the substrate hydrophilicity was possibly masked by unsatisfactory water contact angle measurements by drop shape analysis, as indicated by the lack of consistency between two instruments.

The influence of the nature of the suspending medium of soiling particles will be considered now. In the above example, removal of chromium oxide particles from poly(vinyl chloride) was not influenced by the presence of triolein in the soiling suspension (Pesonen-Leinonen et al., 2006b). In the study of the adherence of starch granules (Detry et al., 2011), SEM micrographs obtained with the in-lens detector showed that macromolecules or sub-micrometer size starch fragments were adsorbed from the liquid phase and, or carried by the liquid film retracting during drying, and were accumulated at the granule-substrate interface. SEM micrographs with in-lens and external detectors were obtained here on soils formed on the two substrates, bare or conditioned with dextran or BSA, using quartz suspension in water or in dextran or BSA solutions, without rinsing. Figure 7 shows a representative micrograph, obtained on a quartz aggregate present on polystyrene conditioned with dextran and soiled with a quartz suspension in dextran solution. The micrographs did not demonstrate any accumulation of macromolecules in or around the aggregates, presumably owing to the low concentration in the solution.

The influence of BSA on glass cleanability, whether it was brought by glass conditioning or by the quartz suspension, is not in accordance with the only influence of the contact angle

discussed above in the comparison between non-conditioned glass and polystyrene. The domination of BSA at interfaces, which was demonstrated by XPS, was found to improve markedly the glass cleanability (Figure 1B, glass) although the contact angle (Figure 3B, glass) and particles distribution (Figure 2) did not change appreciably. On the other hand, conditioning polystyrene with BSA markedly decreased the water contact angle (Figure 3B, polystyrene), which led to more flat aggregates (Figure 2), but this was not correlated with a significance change of cleanability (Figure 1B, polystyrene).

Actually, the key to explain cleanability seems to be the strength of capillary forces developed in the course of drying, which depend on both the contact angle and the liquid surface tension. Assuming that spherical particles are at a small distance of the substrate surface and considering a bridge of liquid forming a ring around the contact point, the capillary forces created by meniscuses between a quartz particle and the substrate can be evaluated by the following equations (Rabinovich et al., 2002; Pitois et al., 2000):

$$F_{CAP} = 4\pi\gamma_L R\cos\left(\frac{\theta_P+\theta_S}{2}\right)\cos\left(\frac{\theta_S-\theta_P}{2}\right) \quad (9)$$

where F_{CAP} is the capillary force (N), γ_L is the liquid surface tension (N/m), R is the soil particle radius (m), θ_S and θ_P are the contact angles of the liquid on the substrate and on the particles, respectively. Capillary forces were computed considering quartz particles of 9 µm radius, a particle contact angle θ_P in the range of 10 to 20° as measured for glass, and surface tensions of 72.2 and 48.7 mN/m for water and for the supernatant of quartz suspensions in BSA solution, respectively (Table 1). The results for F_{CAP} are as follows for situations differing according to the liquid and a range of contact angles:

- water suspension, θ_S 10 to 20°, relevant for glass: F_{CAP} = 8.0 to 7.7 µN;
- BSA-containing suspension, θ_S 10 to 20°, relevant for glass: F_{CAP} = 5.4 to 5.2 µN;
- water suspension, θ_S 75 to 80°, relevant for non-conditioned polystyrene: F_{CAP} = 5.1 to 4.5 µN;
- BSA-containing suspension, θ_S 25 to 30°, relevant for BSA-conditioned polystyrene: F_{CAP} = 5.2 to 5.0 µN.

Note that the hypotheses regarding particle size and shape are not critical if the results are only used for comparison with each other. It appears that the lower cleanability of glass soiled with a quartz suspension in water is due to higher capillary forces developed during drying. The similarity between the cleanability of glass soiled with a BSA-containing suspension and

the cleanability of polystyrene soiled in absence of BSA is due to the combination of contact angle and liquid surface tension in Eq. (9).

Glass soiled with a suspension of quartz particles in water deserves a special comment. The higher cleanability of the conditioned glass compared to the non-conditioned glass (Figure 1B, b compared to a), for similar contact angles (Figure 3B), indicates that, for conditioned glass, the capillary forces were governed by a lower liquid surface tension, due to BSA desorption into the soiling droplets.

The influence of contact angle deserves also some comments. Consider the case of non-conditioned polystyrene soiled with a BSA-containing suspension. If the contact angle governing the capillary forces was in the range of 75 to 85° as measured (Figure 3B, c) F_{CAP} would be in the range of 3.4 to 2.8 µN. The cleanability would thus be expected to be significantly higher than that of BSA-conditioned polystyrene, which is not the case (Figure 1B, c compared to d). Actually the contact angle governing the capillary forces should be the receding contact angle, while the values reported in Figure 3 were measured using the sessile drop method, i.e. close to advancing conditions. While this calls for caution regarding the F_{CAP} values computed above, the comparison between bare glass soiled with a water suspension (receding contact angle below 10°) and bare polystyrene soiled with a water suspension (receding contact angle about 70°, leading to computed F_{CAP} = 5.3 µN) is still valid. Attempts made to measure receding water contact angles of a BSA solution using the Wilhelmy plate method failed to give accurate results, because of perturbations due the weight of a layer of liquid carried along by the substrate as it was withdrawn from the solution (to be published), but this revealed a low contact angle. For BSA-conditioned substrates soiled with a suspension in water, the use of Eq. (9) is further complicated by the uncertainty regarding the liquid surface tension, which depends on the extent of by BSA desorption.

It turns out that the role of capillary forces, which depend directly on both liquid surface tension and contact angle, is more important than the size and shape of the aggregates, which depend on droplet spreading and are thus governed directly by contact angle and only indirectly by liquid surface tension. Eq. (9) is a useful tool to roughly foresee the influence of liquid surface tension, contact angle and their combination. For a given liquid surface tension, the capillary forces will not be reduced by more than 20%, with respect to perfectly wetting surfaces (contact angle close to zero), if the contact angles of the facing surfaces do not exceed the paired values of 10 – 50, 20 – 45, 30 – 40. According to the symmetry properties of Eq. (9), it thus not matter whether the pair is taken as particle – substrate or substrate – particle.

The above discussion is consistent with the fact that the cleanability of glass or polystyrene was not markedly affected by the presence of dextran, as neither the liquid surface tension nor the contact angle was appreciably affected. Moreover dextran was readily desorbed in the presence of water.

5. Conclusion

The interpretation of XPS data by using peak decomposition was validated by correlations between spectral data of independent nature related to peak intensity and peak shape, respectively. The complexity due to the ubiquitous presence of organic contaminants could be coped with, and the surface compositions could be expressed both in terms of the amount of adlayer and mass composition of the adlayer constituents.

When soiled with a suspension of particles in water, glass was much less cleanable than polystyrene, in agreement with the previous observations on starch soil. The presence of dextran did not affect the cleanability of glass or polystyrene. The presence of BSA at the interface improved strongly the cleanability of glass while the contact angle did not change appreciably. In contrast, soiling polystyrene with quartz particles suspended in a BSA solution instead of water did not change markedly the cleanability, while the contact angle was much lower. These observations are explained by the major role of capillary forces developed upon drying, which influence the closeness of the contact between the soiling particles and the substrate and, thereby, the adherence of particles. The capillary forces are proportional to the liquid surface tension but are not expected to be reduced by more than 20%, with respect to perfectly wetting surfaces (contact angle close to zero), if the contact angles of the facing surfaces do not exceed paired values of about 10 – 50, 20 – 45 or 30 – 40. The dependence of cleanability on capillary forces is predominant compared with its dependence on the size and shape of the soiling aggregates, which influence the efficiency of shear forces exerted by the flowing water upon cleaning.

Acknowledgements

This study was supported by the Walloon Region. The support of National Foundation for Scientific Research (FNRS, Belgium) is also gratefully acknowledged. The authors thank Adriaensen Yasmine for the XPS experiments and Sylvie Derclaye for the SEM examinations.

References

Almeida, A. T., Salvadori, M. C., Petri, D. F. S., Box, P. O. (2002). Enolase adsorption onto hydrophobic and hydrophilic solid substrates. *Langmuir, 18*, 6914–6920.

Blel, W., Bénézech, T., Legentilhomme, P., Legrand, J., Le Gentil-Lelièvre, C. (2007). Effect of flow arrangement on the removal of Bacillus spores from stainless steel equipment surfaces during a Cleaning In Place procedure. *Chem. Eng. Sci.*, *62*(14), 3798–3808.

Blel, W., Legentilhomme, P. , Le Gentil-Lelièvre, C. , Faille, C., Legrand, J. B. T. (2010). Cleanability study of complex geometries: Interaction between B. cereus spores and the different flow eddies scales. *Biochem. Eng. J.*, *49*(1), 40–51.

Boonaert, C. J. P., Rouxhet, P. G. (2000). Surface of lactic acid bacteria : relationships between chemical composition and physicochemical properties. *Appl. Environ. Microbiol.*, *66*(6), 2548–254.

Caccavo Jr., F. (1999). Protein-mediated adhesion of the dissimilatory Fe (III) - Reducing bacterium *Shewanella* alga BrY to hydrous ferric oxide. *Appl. Environ. Microbiol.*, *65*(11), 5017–5022.

Caillou, S., Boonaert, C. J. P., Dewez, J., Rouxhet, P. G. (2007). Oxidation of proteins adsorbed on hemodialysis membranes and model materials. *J. Biomed. Mater. Res. Part B Appl. Biomater.*, *84B*(1), 240–248.

Detry, J. G, Sindic, M., Servais, M. J., Adriaensen, Y., Derclaye, S., Deroanne, C., Rouxhet, P. G. (2011). Physico-chemical mechanisms governing the adherence of starch granules on materials with different hydrophobicities. *J. Colloid Interface Sci.*, *355*(1), 210–21.

Detry, J. G., Jensen, B. B. B., Sindic, M., Deroanne, C. (2009a). Flow rate dependency of critical wall shear stress in a radial-flow cell. *J. Food Eng.*, *92*(1), 86–99.

Detry, J.G., Deroanne, C., Sindic, M., Jensen, B. B. B. (2009b). Laminar flow in radial flow cell with small aspect ratios: Numerical and experimental study. *Chem. Eng. Sci.*, *64*(1), 31–42.

Detry, J. G., Rouxhet, P. G., Boulangé-Petermann, L., Deroanne, C., Sindic, M. (2007). Cleanability assessment of model solid surfaces with a radial-flow cell. *Colloids Surfaces A. Physicochem. Eng. Asp.*, *302*(1-3), 540–548.

Dufrêne, Y. F., Boonaert, C. J. P, Rouxhet G. P. (1996). Adhesion of *Azospirillum brasilense* : role of proteins at the cell-support interface. *Colloids Surfaces B. Biointerfaces*, *7*, 113–128.

Dupont-Gillain, C. C., Mc Evoy, K. M., Henry, M., Bertrand, P. (2010). Surface spectroscopy of adsorbed proteins: input of data treatment by principal component analysis. *J. Mater. Sci. Mater. Med.*, *21*(3), 955–61.

Dupont-Gillain, C. C., Adriaensen, Y., Derclaye, S., Rouxhet, P. G. (2000). Plasma-oxidized polystyrene : wetting properties and surface reconstruction. *Langmuir, 16*, 8194-8200

Flint, S. H., Brooks, J. D., Bremer, P. J. (1997). The influence of cell surface properties of thermophilic streptococci on attachment to stainless steel. *J. Appl. Microbiol.*, *83*(4), 508–517.

Fryer, P. J., Asteriadou, K. (2009). A prototype cleaning map: A classification of industrial cleaning processes. *Trends Food Sci. Technol.*, *20*(6-7), 255–262.

Gerin, P.A., Dengis, P.B., Rouxhet, P.G (1995). Performance of XPS analysis of model biochemical compounds. *J. Chim. Phys.*, *92*(5), 1034–1065.

Goldstein, A. S., DiMilla, P. A. (1998). Comparison of converging and diverging radial flow for measuring cell adhesion. *AIChE J.*, *44*(2), 465–473.

Goldstein, A S, DiMilla, P. A. (1997). Application of fluid mechanic and kinetic models to characterize mammalian cell detachment in a radial-flow chamber. *Biotechnol. Bioeng.*, *55*(4), 616–29.

Hirayama, K., Akashi S, Furuya, M., Furuya, K. (1990). Rapid confirmation and revision of the primary structure of bovine serum albumin by ESIMS and Frit-FAB LC/MS. *Biochem. Biophys. Res. Commun., 173*(2), 639-646.

Jensen, B. B. B., Friis, A. (2004). Critical wall shear stress for the EHEDG test method. *Chem. Eng. Process. Process Intensif.*, *43*(7), 831–840.

Jensen, B. B. B., Stenby, M., Nielsen, D. F. (2007). Improving the cleaning effect by changing average velocity. *Trends Food Sci. Technol.*, *18*, S58–S63.

Jensen, B. B. B., Friis, A., Bénézech, T., Legentilhomme, P., Lelièvre, C. (2005). Local wall shear stress variations predicted by computational fluid dynamics for hygienic design. *Food Bioprod. Process.*, *83*(1), 53–60.

Kopac, T., Bozgeyik, K., Yener, J. (2008). Effect of pH and temperature on the adsorption of bovine serum albumin onto titanium dioxide. *Colloids Surfaces A. Physicochemical Eng. Asp.*, *322*(1-3), 19–28.

Kosaka, P. M., Kawano, Y., Salvadori, M. C., Petri, D. F. S. (2005). Characterization of ultrathin films of cellulose esters. *Cellulose*, *12*(4), 351–359.

Kralchevsky, P. A, Denkov, N. D. (2001). Capillary forces and structuring in layers of colloid particles. *Curr. Opin. Colloid Interface Sci.*, *6*(4), 383–401.

Kralchevsky, P. A., Nagayama, K. (2001). Lateral capillary forces between partially immersed bodies. *Elsevier, Amsterdam*, 287–350.

Kralchevsky, P. A., Nagayama, K. (1994). Capillary forces between colloidal particles. *Langmuir*, *10*(1), 23–36.

Kuisma, R., Fröberg, L., Kymäläinen, H.-R., Pesonen-Leinonen, E., Piispanen, M., Melamies, P., Hautala, M., Sjöberg, A-M., & Hupa, L. (2007). Microstructure and cleanability of uncoated and fluoropolymer, zirconia and titania coated ceramic glazed surfaces. *J. Eur. Ceram. Soc.*, *27*(1), 101–108.

Lelièvre C., Legentilhomme, P. Gaucher, C., Legrand, J., Faille, C., Bénézech, T. (2002). Cleaning in place : effect of local wall shear stress variation on bacterial removal from stainless steel equipment. *Chem. Eng. Sci.*, *57*, 1287–1297.

Lower, B. H., Yongsunthon, R., Iii, F. P. V., Lower, S. K. (2005). Simultaneous force and fluorescence measurements of a protein that forms a bond between a living bacterium and a solid surface. *J. Bacteriol.*, *187*(6), 2127–2137.

Määttä, J., Piispanen, M., Kuisma, R., Kymäläinen, H.-R., Uusi-Rauva, A., Hurme, K.-R., Arevad, S., Sjöberg, A.-M, Hupa, L. (2007). Effect of coating on cleanability of glazed surfaces. *J. Eur. Ceram. Soc.*, *27*(16), 4555–4560.

Määttä, J., Kuisma, R., Kymäläinen, H.-R. (2011). Modifications of surface materials and their effects on cleanability as studied by radiochemical methods. *Constr. Build. Mater.*, *25*(6), 2860–2866.

Mauermann, M., Eschenhagen, U., Bley, T., Majschak, J. P. (2009). Surface modifications – Application potential for the reduction of cleaning costs in the food processing industry. *Trends Food Sci. Technol.*, *20*, S9–S15.

Mauermann, M., Calvimontes, A., Bellmann, C., Simon, F., Schöler M., Majschak, J. P. (2011). Modifications in hygienic properties of stainless steel surfaces due to repeated soiling and cleaning. *Proc. Int. Conf. Heat Exch. Fouling Clean.*, *IX*, 227–234.

Mercier-Bonin, M., Adoue, M., Zanna, S., Marcus, P., Combes, D., Schmitz, P. (2009). Evaluation of adhesion force between functionalized microbeads and protein-coated stainless steel using shear-flow-induced detachment. *J. Colloid Interface Sci.*, *338*(1), 73–81.

Norde, W., Giacomelli, C. E. (2000). BSA structural changes during homomolecular exchange between the adsorbed and the dissolved states. *J. Colloid Interface Sci.*, *79*(3), 259–68.

Pesonen-Leinonen, E., Kuisma, R., Redsven, I., SJOBERG, A., Hautala, M. (2006a). Can contact angle measurements be used to predict soiling and cleaning of plastic flooring

materials? In *Contact angle, wettability and adhesion (*K. L. Mittal, ed.) Vol. 4, VSP/Brill, Leiden, 203–214.

Pesonen-Leinonen, E., Redsven, I., Neuvonen, P., Hurme, K.-R., Pääkko, M., Koponen, H.-K., Pakkanen, T.T., Uusi-Rauva, A., Hautala, M., Sjöberg, A.-M. (2006b). Determination of soil adhesion to plastic surfaces using a radioactive tracer. *Appl. Radiat. Isot.*, *64*(2), 163–169.

Piispanen, M., Kronberg, T., Areva, S., Hupa, L. (2011). Effect of mechanical and chemical wear on soil attachment and cleanability of sanitary ware with additional coatings. *J. Am. Ceram. Soc.*, *94*(3), 951–958.

Pitois, O., Moucheront, P., Château, X. (2000). Liquid bridge between two moving spheres: an experimental study of viscosity effects. *J. Colloid Interface Sci. 231*(1), 26–31.

Podczeck, F. (1999). Investigations into the reduction of powder adhesion to stainless steel surfaces by surface modification to aid capsule filling. *Int. J. Pharm.*, *178*(1), 93–100.

Rabinovich, Y. I, Adler, J. J., Esayanur M. S., Ata, A., Singh, R., Moudgil, B. M. (2002). Capillary forces between surfaces with nanoscale roughness. *Adv. Colloid Interface Sci. 96*(1-3), 213–30.

Rouxhet, G. P., Misselyn-Bauduin, A. M., Ahimou, F., Genet, M. J., Adriaensen, Y., Desille, T., Bodson, P., Deroanne, C. (2008). XPS analysis of food products: toward chemical functions and molecular compounds. *Surf. Interface Anal.*, *40*(3-4), 718–724.

Rouxhet, G. P. (2013). Contact angles and surface energy of solids: Relevance and limitations, in *Advances in contact angle, wettability and adhesion.*(K. L. Mittal, ed.) Vol. 1, Schrivener Publishing LLC, 347-375

Rouxhet, G. P., Genet, M. J. (2011). XPS analysis of bio-organic systems. *Surf. Interface Anal.*, *43*(12), 1453–1470.

Speranza, G., Gottardi, G., Pederzolli, C., Lunelli, L., Canteri, R., Pasquardini, L., Carli, E., Lui, A., Maniglio, D., Brugnara, M., Anderle, M. (2004). Role of chemical interactions in bacterial adhesion to polymer surfaces. *Biomaterials*, *25*(11), 2029–2037.

Stephan, O., Weisz, N., Vieths, S., Weiser, T., Rabe, B., Vatterott, W. (2004). Protein quantification, sandwich ELISA, and real-time PCR used to monitor industrial cleaning procedures for contamination with peanut and celery allergens. *J. AOAC Int.*, *87*(6), 1448–1457.

Thill, A., Spalla., O (2003). Aggregation due to capillary forces during drying of particle submonolayers. *Colloids Surfaces A. Physicochem. Eng. Asp.*, *217*(1-3), 143–151.

Tomasetti, E., Derclaye, S., Delvaux, M.H. and Rouxhet, P.G. (2013) Study of material-water interactions using the Wilhelmy plate method, in *Advances in contact angle, wettability and adhesion.*(K. L. Mittal, ed.) Vol. 1, Schrivener Publishing LLC, 131-154.

Touré, Y., Rouxhet P. G. and Sindic, M.. (2013). Influence of soluble proteins on the adherence of particulate soils. *Ref. Proc. Int. Conf. Heat Exch. Fouling Clean.*, *X*, 285–90.

Touré ,Y., Rouxhet P. G., Dupont-Gillain, C. C., Sindic, M. (2011). Influence of soluble polysaccharide on the adherence of particulate soils. *Ref. Proc. Int. Conf. Heat Exch. Fouling Clean.*, *IX*, 219–226.

Walstra, P., Jenness, R. (1984). *Dairy chemistry and physics*. John Wiley and Sons, New York.

Yang, J., Mcguire J., Kolbe E. R. (1991). Use of the equilibrium contact angle as an index of contact surface cleanliness. *J. Food Prot.*, *54*(11), 879–884.

Figure captions

Figure 1. Critical detachment radius measured on bare substrates (a, c) and on substrates conditioned with macromolecules (b, d), soiled with quartz particles suspensions in water (a, b), or in a solution of macromolecules (c, d). The macromolecules were dextran (A) or BSA (B).

Figure 2. Micrographs of glass (A) and polystyrene (B) surfaces conditioned or not as indicated, and soiled with quartz particles suspensions in water, dextran solution or BSA solution, as indicated. Top line in A and B, optical micrographs (scale bar 300 µm); middle line in B, same obtained by image analysis with a threshold of 180; bottom line in A and B, SEM micrographs made with the external detector (scale bar 200 µm).

Figure 3. Contact angle measured on bare substrates (a, c, e) and on substrates conditioned with macromolecules (b, d, f), using the supernatant of quartz suspensions in water (a, b), or the supernatant of quartz suspensions in solutions of macromolecules (c, d), or using a solution of macromolecules (e, f). The macromolecules were dextran (A) or BSA (B).

Figure 4. Representative O 1s, N 1s and C 1s peaks recorded on quartz powder and glass substrate, conditioned or not with dextran and BSA, and illustration of C 1s peak decomposition.

Figure 5. Correlations between the indicated sums of concentrations regarding the elemental nature of carbon (mole fraction of elements): BSA (✱, only in a and b); dextran (×, only in c); glass (●,○), polystyrene (■,□, only in a) and quartz powder (▲,△), bare (closed symbols) or conditioned and rinsed (open symbols) or conditioned and not rinsed (open symbols with dot). a and b, substrate conditioning with BSA; c, substrate conditioning with dextran. Dashed line: regression line with its equation; in a this was computed excluding the non-conditioned solids.

Figure 6. Correlations between the concentration of inorganic oxygen, evaluated from Equ. (4), and the weighted sum of Si and Na concentrations (mole fraction of elements) for the siliceous solids: glass (●,○), quartz powder (▲,△), bare (closed symbols) or conditioned with BSA (open symbols) or conditioned with dextran (open symbols with dot). Dashed line: regression line with its equation.

Figure 7. SEM micrograph (in-lens detector; scale bar 20µm) recorded on an aggregate present on polystyrene conditioned with dextran and soiled with a suspension of quartz particles in dextran solution.

Table 1. Surface tension (mN/m) of water, of solutions (8 g/L) of dextran and BSA and of supernatants of suspensions of quartz particles in water, dextran solution or BSA solution.

Water	Solution		Supernatant of quartz particles		
	Dextran	BSA	in water	in dextran solution	in BSA solution
72.2 ± 1.1*	72.8 ± 0.1	30.0 ± 1.1	72.9 ± 0.3	68.6 ± 1.1	48.7 ± 2.3

*Mean ± standard deviation

Table 2. Surface concentration (mole fraction with respect to all elements except hydrogen, in %) measured by XPS on dextran, BSA, bare substrates and conditioned substrates, rinsed (1, 2, 3 or 4 times) or not, quartz powders collected from suspension in water, or in dextran or BSA solution: elements and carbon present in different functions associated to C 1s peak components. The results for quartz powders involving 3 rinsing steps, on the one hand, and 2 and 4 rinsing steps, on the other hand, are from independent experiments.

			Mole fraction of element (%)						Mole fraction of carbon (%)				
Element, function			**C**	**O**	**N**	**Si**	**S**	**Na**	**C-(C,H)**	**C-(O,N)**	**N-C=O O-C-O**	**O-C=O**	**Shake up**
Binding energy (eV)									284.8	286.3	288.0	289.3	291.4
Dextran			62.8	35.3	1.6	0.3	n.m.	n.m.	18.0	35.5	8.4	1.0	
BSA			67.3	17.9	13.9	b.d.l	0.5	0.4	37.4	16.1	13.8	b.d.l.	
Solid	**condit.**	**rinse**											
Glass	none		17.5	58.4	0.0	22.3	n.m.	1.9	12.2	3.1	1.2	1.0	
Powder	none		7.0	63.5	0.0	29.5	n.m.	n.m.	4.8	1.3	0.6	0.3	
Glass	dextran	none	39.0	49.2	0.2	10.1	n.m.	1.6	8.7	23.7	6.1	0.6	
Glass	dextran	none	54.0	45.2	0.1	0.5	n.m.	0.2	5.3	39.0	9.1	0.6	
Glass	dextran	1	16.5	61.1	0.1	21.8	n.m.	0.5	8.9	5.6	1.5	0.5	
Glass	dextran	3	18.2	59.5	0.3	21.5	n.m.	0.5	11.3	4.8	1.5	0.6	
Powder	dextran	none	23.7	57.5	0.0	18.9	n.m.	n.m.	3.3	16.3	3.6	0.5	
Powder	dextran	3	6.6	62.2	0.3	30.9	n.m.	n.m.	4.7	1.3	0.6	b.d.l.	
Powder	dextran	none	20.2	59.9	0.0	19.9	n.m.	n.m.	3.5	13.5	2.9	0.3	
Powder	dextran	2	7.2	67.3	0.0	25.5	n.m.	n.m.	5.7	1.1	b.d.l.	0.5	
Powder	dextran	4	7.0	67.4	0.0	25.5	n.m.	n.m.	5.5	1.2	b.d.l.	0.3	
Glass	BSA	none	63.1	20.5	15.0	0.8	n.m.	0.5	30.3	18.3	14.2	0.3	
Glass	BSA	none	53.3	27.1	12.0	6.1	0.4	1.0	26.8	14.7	11.2	0.7	
Glass	BSA	1	45.3	33.9	10.3	9.3	0.2	1.0	23.6	12.3	9.1	0.2	
Glass	BSA	3	42.9	35.5	9.4	10.8	0.2	1.2	22.5	11.0	8.8	0.5	
Powder	BSA	none	28.1	45.1	6.7	20.1	n.m.	n.m.	14.0	7.9	6.2	b.d.l.	
Powder	BSA	3	40.3	35.9	10.4	13.4	n.m.	n.m.	19.1	12.2	9.0	b.d.l.	
Powder	BSA	none	34.5	41.8	8.6	15.1	n.m.	n.m.	17.2	10.0	7.3	b.d.l.	
Powder	BSA	2	27.2	47.0	6.6	19.2	n.m.	n.m.	13.5	8.0	5.7	b.d.l.	
Powder	BSA	4	31.5	44.1	7.2	17.2	n.m.	n.m.	17.3	7.6	6.6	b.d.l.	
Polystyrene	none		94.9	3.5	0.0	1.7	n.m.	n.m.	86.3	2.5	b.d.l.	b.d.l.	6.0
Polystyr.	dextran	none	82.8	12.9	2.4	2.0	n.m.	n.m.	69.0	9.5	2.2	b.d.l.	2.0
Polystyr.	dextran	none	87.0	9.2	1.1	2.7	n.m.	n.m.	76.9	6.1	0.9	b.d.l.	3.1
Polystyr.	dextran	1	80.7	12.9	0.9	5.5	n.m.	n.m.	73.6	4.4	0.4	b.d.l.	2.3
Polystyr.	dextran	3	84.0	10.8	0.6	4.6	n.m.	n.m.	78.6	3.0	b.d.l.	b.d.l.	2.4
Polystyr.	BSA	none	65.6	19.0	14.4	0.3	0.6	0.2	35.7	17.2	12.7	b.d.l.	b.d.l.
Polystyr.	BSA	none	64.7	19.9	14.1	0.3	0.6	0.4	35.6	16.9	12.3	b.d.l.	b.d.l.
Polystyr.	BSA	1	81.8	11.3	5.6	1.2	0.1	b.d.l	63.5	9.0	2.9	3.4	3.0
Polystyr.	BSA	3	80.4	12.4	5.2	1.9	0.1	b.d.l	63.7	8.8	3.9	1.0	3.0

n.m. not measured

b.d.l. below detection limit

Table 3. Surface composition deduced by XPS for bare substrates and conditioned substrates, rinsed (1, 2, 3 or 4times) or not: contributions of the organic adlayer (sum of constituting elements Σads, in mole %) and of the solid (sum of constituting elements Σsol, in mole %) to the XPS spectrum; composition (mass %) of the organic adlayer present on the solids, computed according to two models. The results for quartz powders involving 3 rinsing steps, on the one hand, and 2 and 4 rinsing steps, on the other hand, are from independent experiments.

			Sum of elements (mole %)		Organic composition (mass %)				
					Model A		Model B		
			Adlayer	Solid	Protein	Non protein	Protein	Dextran	Hydrocarbon
Solid	**condit.**	**rinse**							
Glass	none		22.7	69.7	0.0	100.0		n.a.	
Powder	none		9.2	88.4	0.0	100.0		n.a.	
Glass	dextran	none	69.4	32.6	1.8	98.2	1.9	85.8	12.3
Glass	dextran	none	102.7	1.7	0.5	99.5	0.6	94.2	5.2
Glass	dextran	1	24.1	66.1	3.0	97.0	3.1	60.0	36.8
Glass	dextran	3	25.1	65.4	6.1	93.9	6.3	49.9	43.8
Powder	dextran	none	44.1	56.6	0.0	100.0	0.0	92.3	7.7
Powder	dextran	3	8.5	92.6	21.9	78.1	22.3	28.2	49.5
Powder	dextran	none	36.9	59.7	0.0	100.0	0.0	90.2	9.8
Powder	dextran	2	8.8	76.4	0.0	100.0	0.0	34.7	65.3
Powder	dextran	4	8.5	76.6	0.0	100.0	0.0	33.6	66.4
Glass	BSA	none	95.9	3.0	90.4	9.6		n.a.	
Glass	BSA	none	79.9	19.7	87.3	12.7		n.a.	
Glass	BSA	1	66.9	29.5	88.7	11.3		n.a.	
Glass	BSA	3	63.3	34.3	86.1	13.9		n.a.	
Powder	BSA	none	42.2	60.4	91.2	8.8		n.a.	
Powder	BSA	3	61.5	40.2	97.3	2.7		n.a.	
Powder	BSA	none	51.7	45.4	95.8	4.2		n.a.	
Powder	BSA	2	40.8	57.7	93.4	6.6		n.a.	
Powder	BSA	4	45.8	51.6	91.2	8.8		n.a.	
Polystyr.	none		5.1	92.3	n.a.			n.a.	
Polystyr.	dextran	none	28.0	66.9	14.9	85.1*	15.5	14.5	70.0*
Polystyr.	dextran	none	16.3	78.0	7.2	92.8*	7.5	10.2	82.3*
Polystyr.	dextran	1	11.3	74.3	6.6	93.4*	6.8	6.7	86.5*
Polystyr.	dextran	3	7.2	80.0	4.2	95.8*	4.4	4.1	91.5*
Polystyr.	BSA	none	87.2	11.3	87.2	12.8*		n.a.	
Polystyr.	BSA	none	85.3	11.6	87.3	12.7*		n.a.	
Polystyr.	BSA	1	41.3	57.0	34.1	65.9*		n.a.	
Polystyr.	BSA	3	37.4	57.8	33.0	67.0*		n.a.	

n.a not applied

* this includes the contribution of the polystyrene substrate

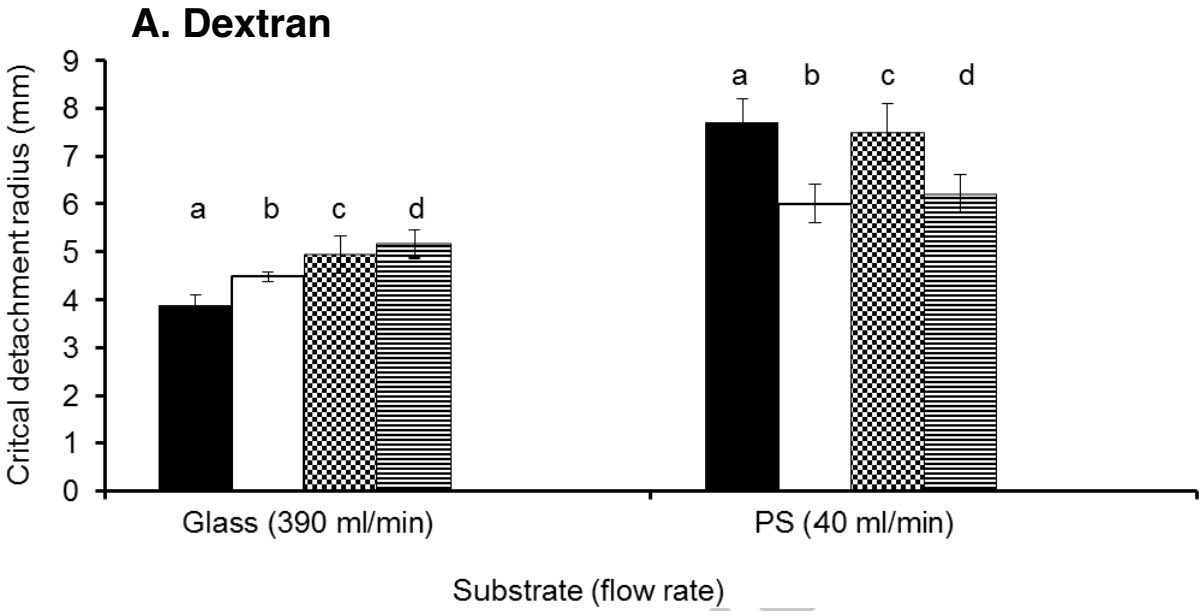

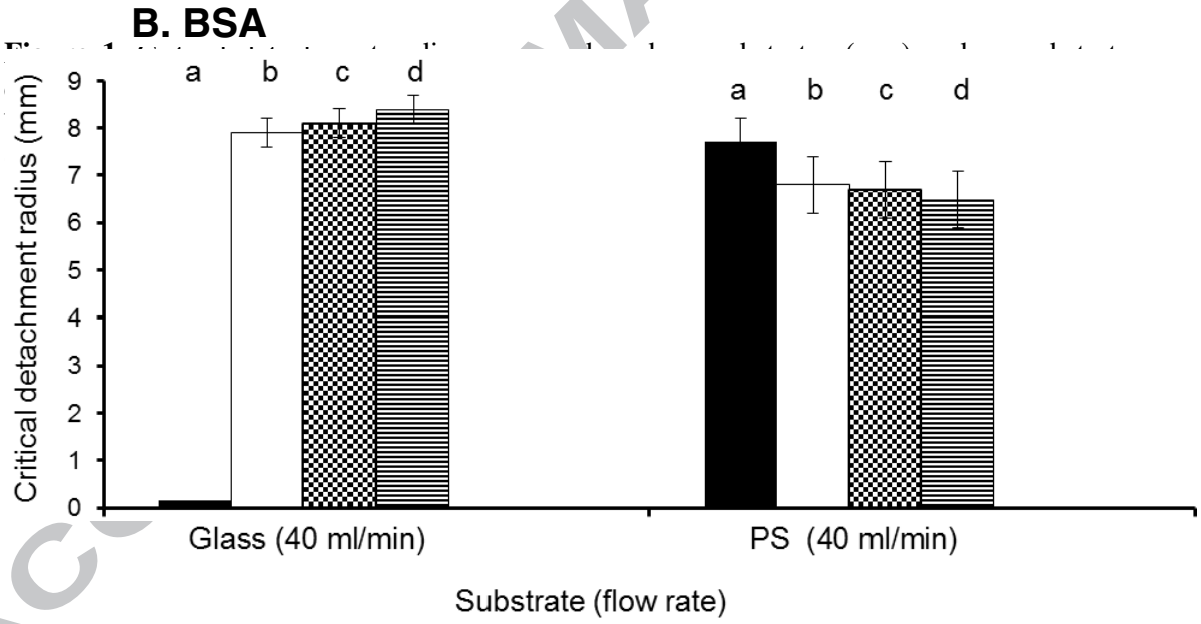

A. Glass

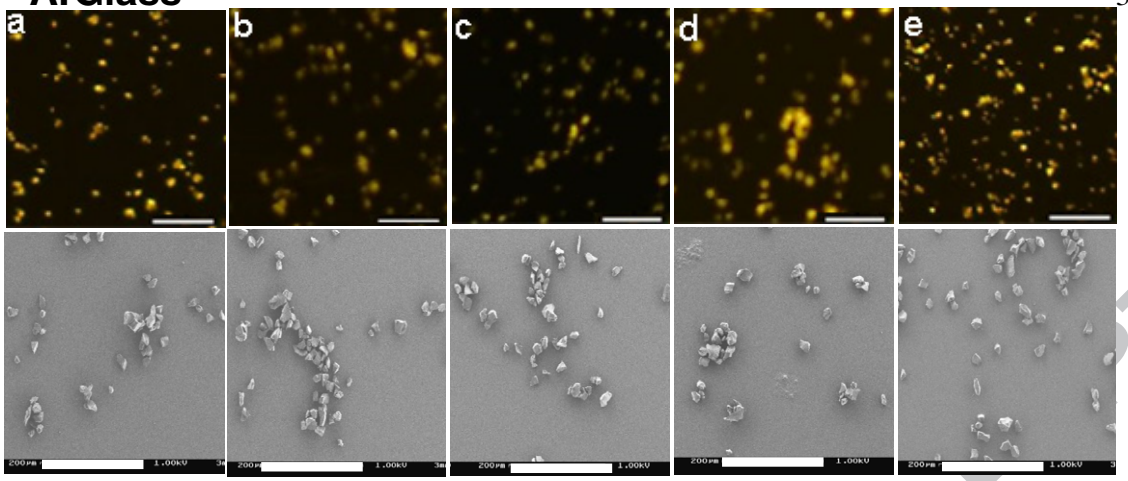

B. Polystyrene

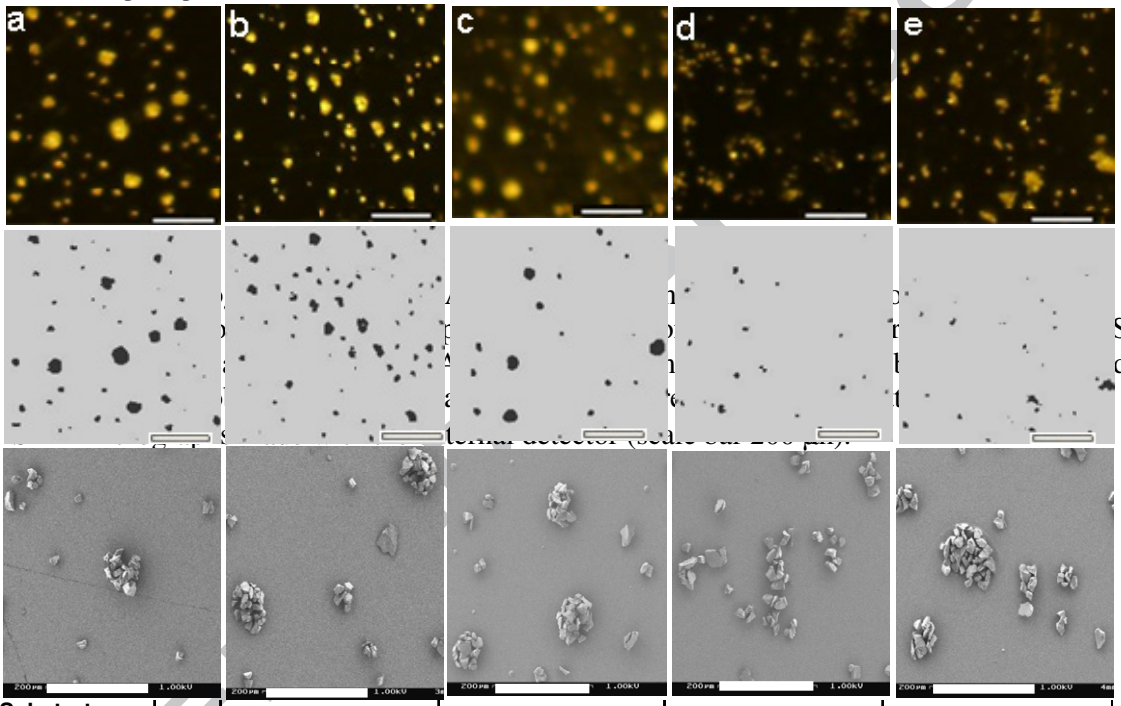

as
SA
dle
B,

Substrate conditioning	none	dextran	none	BSA	none
Quartz suspension in	water	water	dextran solution	none	BSA solution

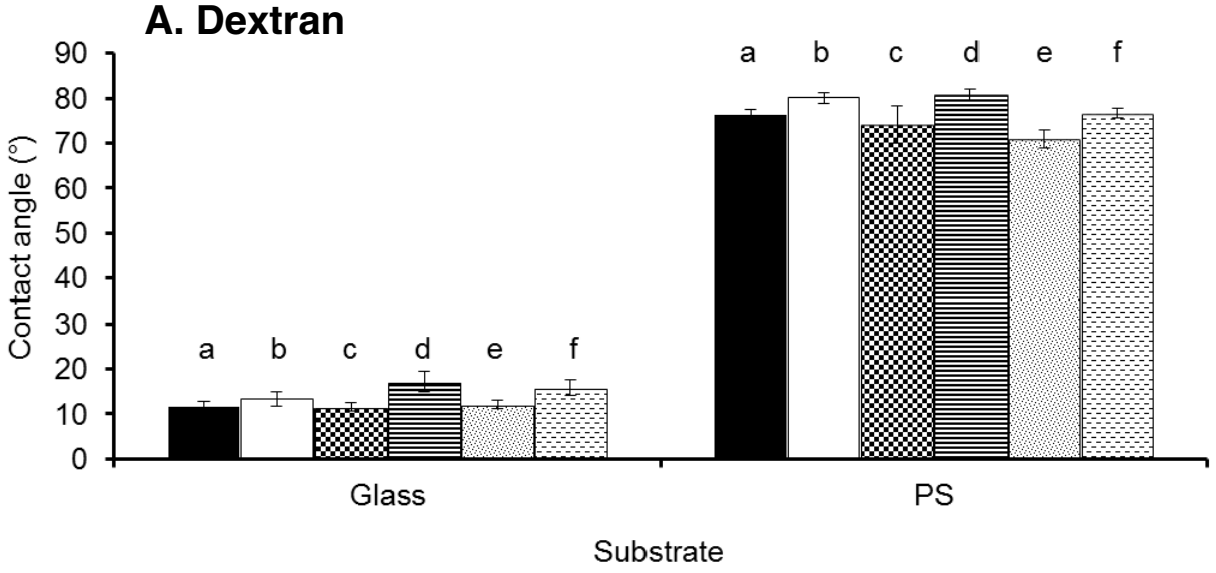

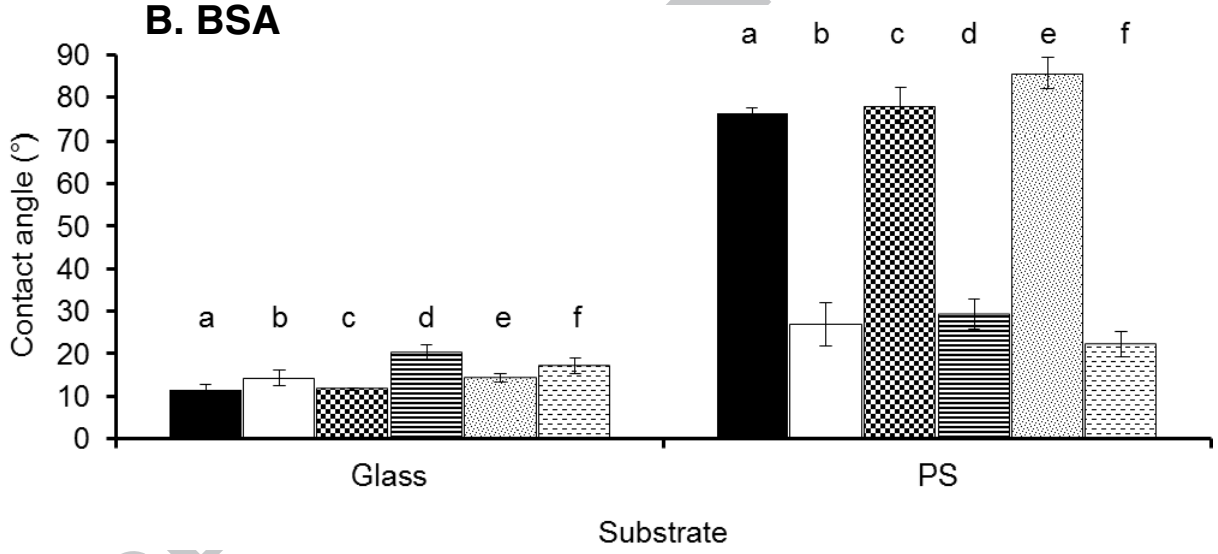

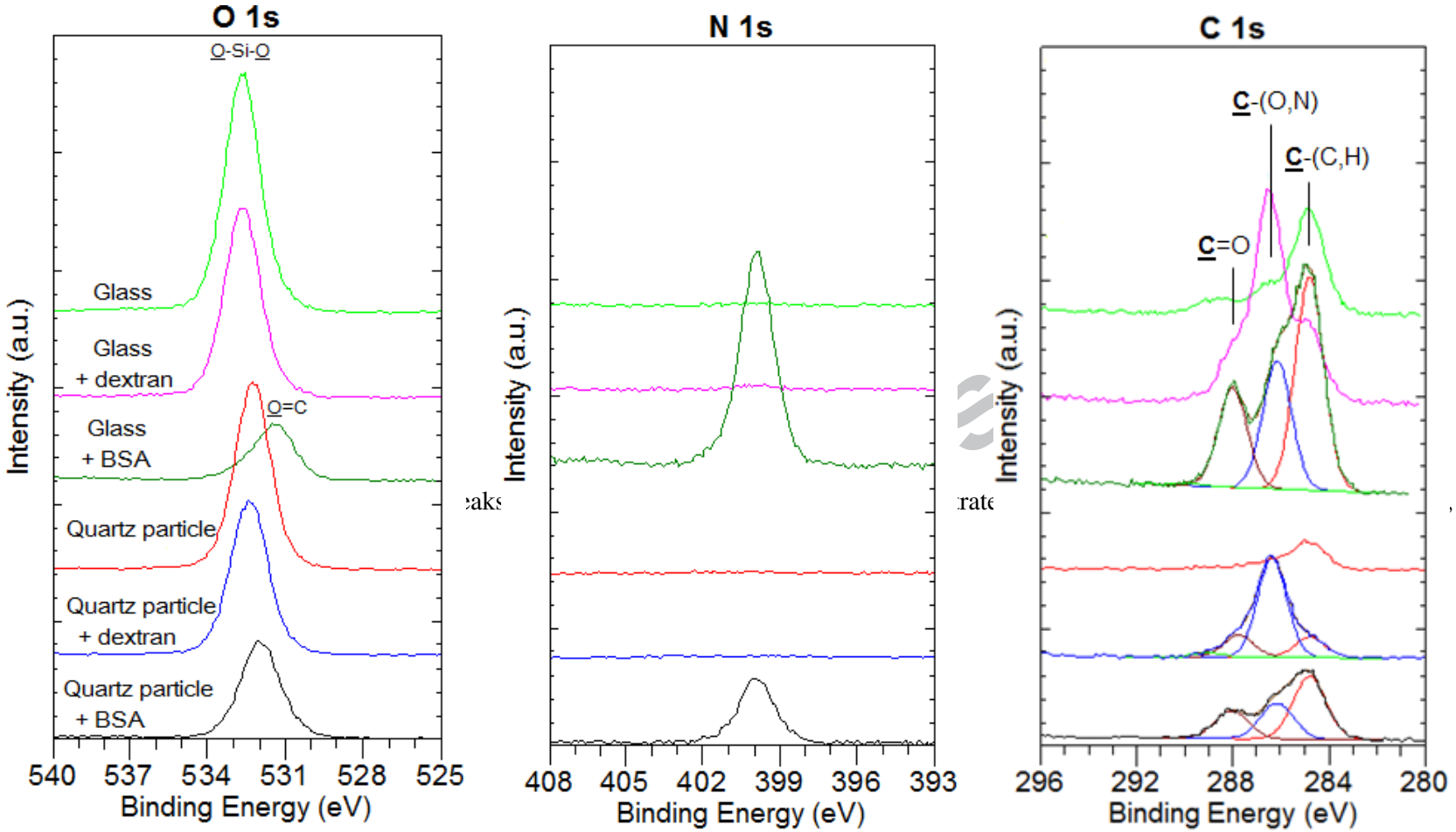

Fig ;aks ;rate
and

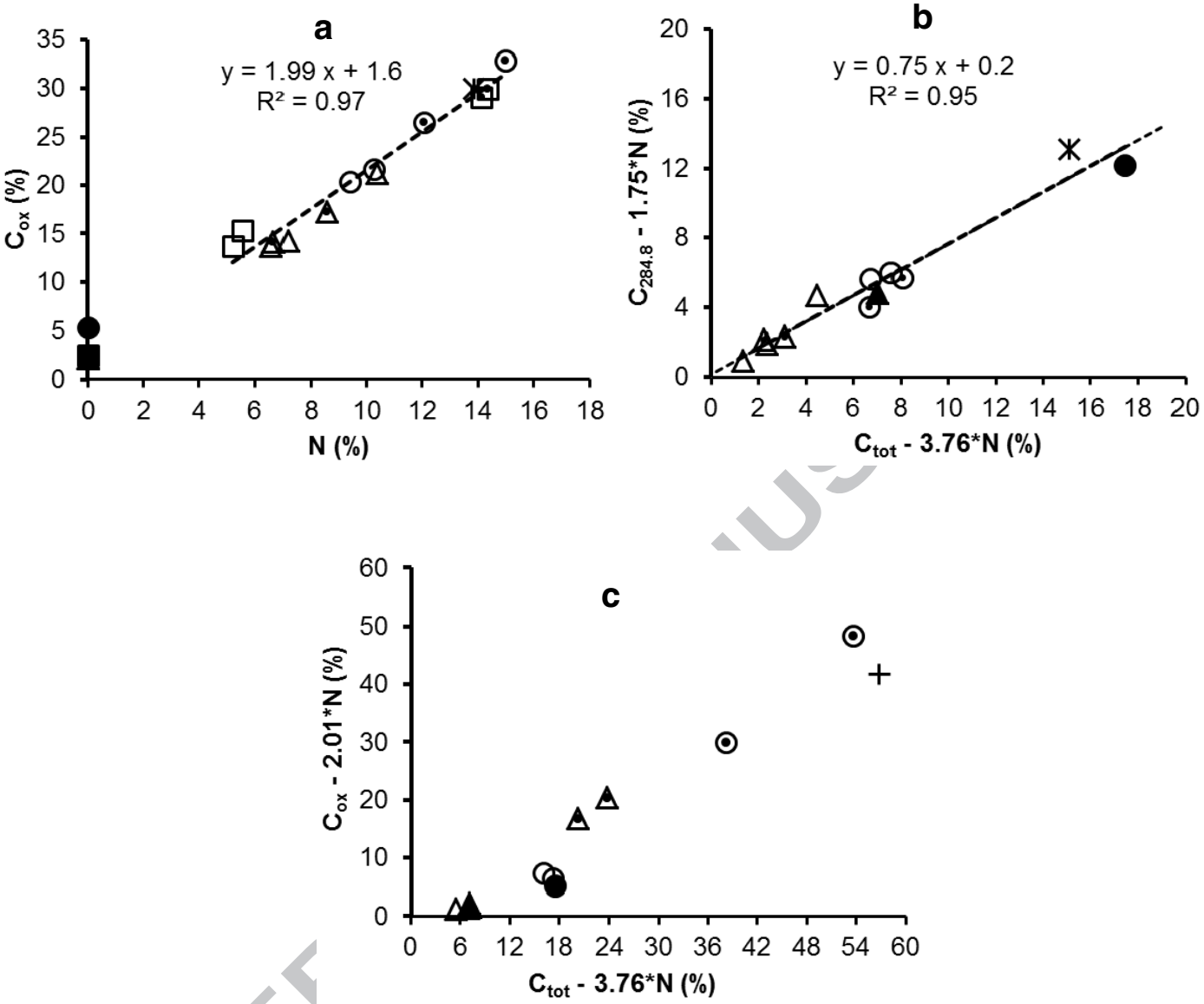

Figure 5. Correlations between the indicated sums of concentrations regarding the elemental nature of carbon (mole fraction of elements): BSA (✱, only in a and b); dextran (✕, only in c); glass (●,○), polystyrene (■,□, only in a) and quartz powder (▲,△), bare (closed symbols) or conditioned and rinsed (open symbols) or conditioned and not rinsed (open symbols with dot). a and b, substrate conditioning with BSA; c, substrate conditioning with dextran. Dashed line: regression line with its equation; in a this was computed excluding the non-conditioned solids.

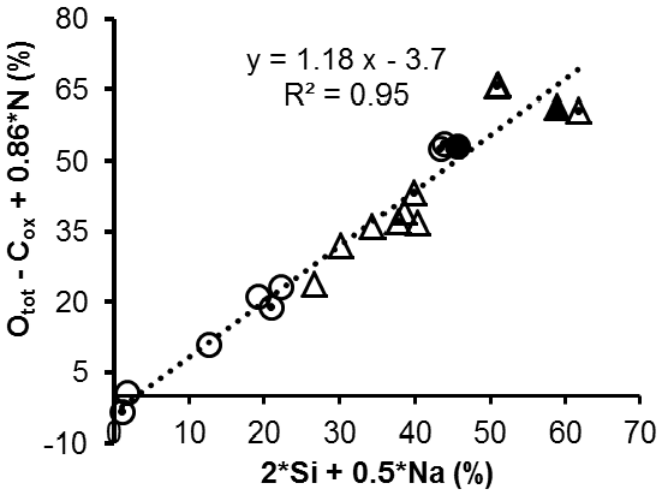

Figure 6. Correlations between the concentration of inorganic oxygen, evaluated from Equ. (4), and the weighted sum of Si and Na concentrations (mole fraction of elements) for the siliceous solids: glass (●,○), quartz powder (▲,△), bare (closed symbols) or conditioned with BSA (open symbols) or conditioned with dextran (open symbols with dot). Dashed line: regression line with its equation.

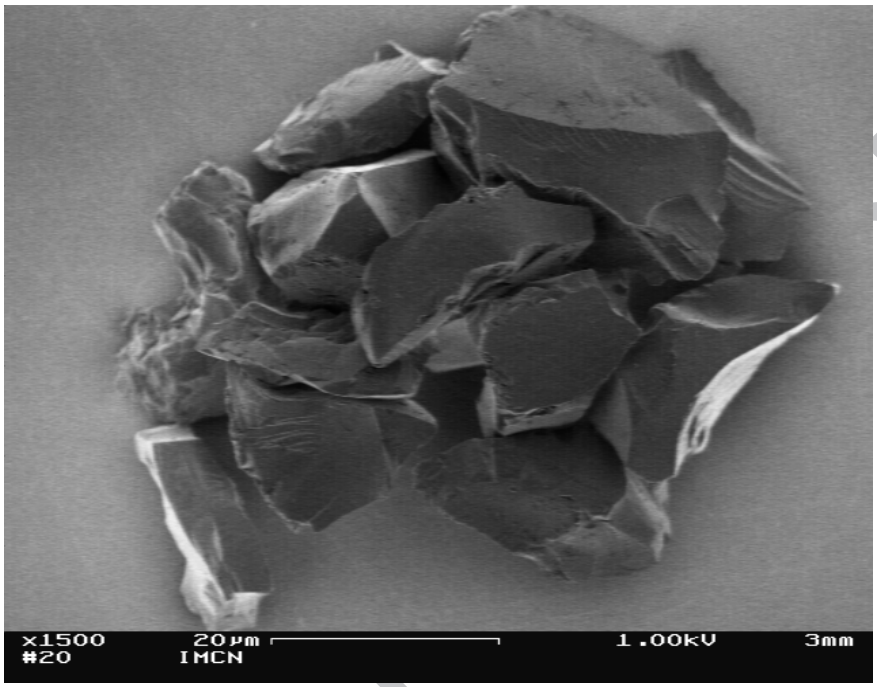

Figure 7. SEM micrograph (in-lens detector; scale bar 20µm) recorded on an aggregate present on polystyrene conditioned with dextran and soiled with a suspension of quartz particles in dextran solution.

Graphical abstract

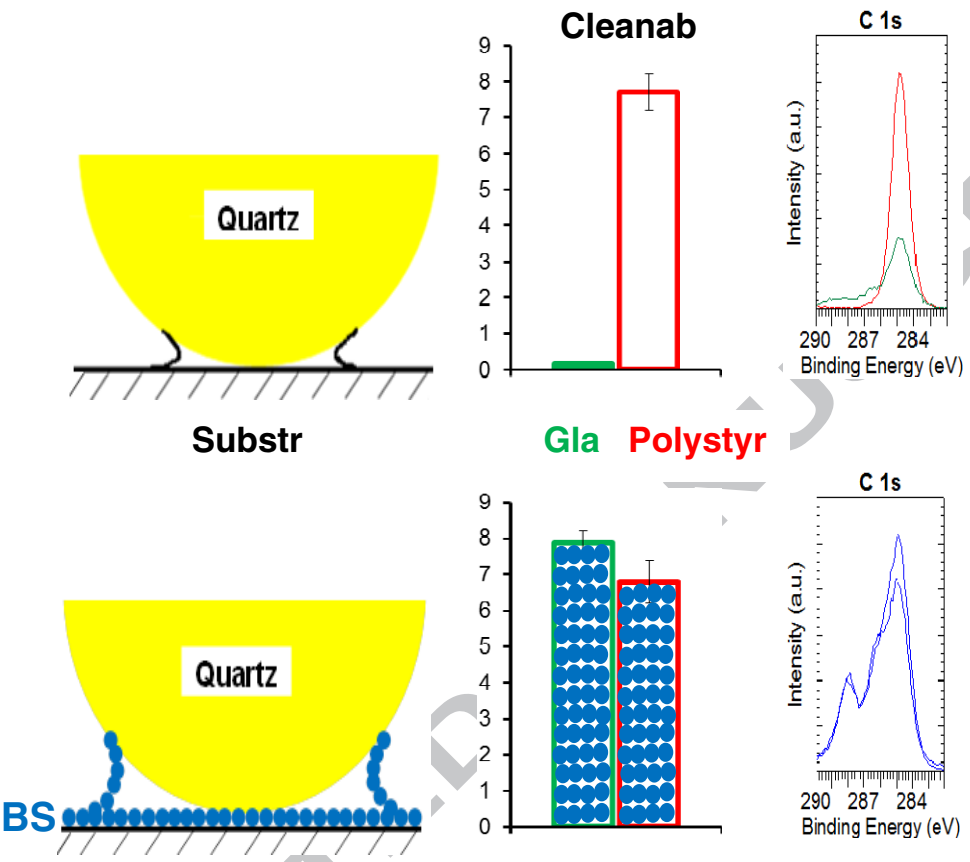

Highlights

Surface composition given by the amount of adlayer and the mass concentration of constituents.

Difference between glass and polystyrene in accordance with expectation based on capillary forces.

BSA improves markedly the cleanability of glass and not of polystyrene.

The influence of BSA is due to lowering of liquid surface tension..

The influence of the size and shape of adhering aggregates on cleanability is of less importance.